A Novel Study of Penetration into Concrete Targets by Ogive Nose Projectiles

A. R. Khoogar*
Department of Mechanical Engineering,
Maleke-Ashtar University of Technology, Tehran, Iran
Email: Khoogar@gmail.com
*Corresponding author

M. A. Mohades
Department of Mechanical Engineering,
Maleke-Ashtar University of Technology, Tehran, Iran.
Email: mohades-ali@yahoo.com

Kh. Vahedi
Department of Mechanical and Aerospace Engineering,
Imam Hosain University, Tehran, Iran

Received: 4 May 2012, Revised: 21 September 2012, Accepted: 29 December 2012

Abstract: In design of defence structures, concrete is often used to provide protection against incidental dynamic loadings such as the impact of a steel projectile. In the present study, a new analytical model is proposed to predict penetration depth into concrete targets by ogive nose projectile. Hence, to develop the model and simulate penetration of high velocity ogive-shape nose steel projectiles into concrete targets, several tests have been simulated numerically with the Ls-Dyna finite element code. The results show good agreement between the developed analytical model and the experimental results from other researchers.

Keywords: Cavity Expansion, Concrete, Fracture, Penetration, Projectile

Reference: Khoogar, A. R., Mohades, M. A., and Vahedi, Kh. "A Novel Study Of Penetration Into Concrete Targets By Ogive Nose Projectiles", Int J of Advanced Design and Manufacturing Technology, Vol. 6/ No. 3, 2013, pp. 1-7.

Biographical notes: Ahmad R. Khoogar received his PhD in Mechanical Engineering from the University of Alabama in 1989. He is currently Assistant Professor at the Department of Mechanical Engineering in the Maleke-Ashtar University of Technology in Tehran. His current research interest includes Robotics and Vibrations. **M. A. Mohades** received his MSc degree in Mechanical engineering from Maleke-Ashtar University of Technology in 2011. His current research interests include high speed fracture mechanics and computational solid mechanics. **Kh. Vahedi** is an Assistant Professor in the Department of Mechanical and Aerospace Engineering in the Imam Hossain University, Tehran.

Archive of SID

© 2013 IAU, Majlesi Branch www.SID.ir

1 INTRODUCTION

Concrete has been used in protective structures for centuries. Because of military interests in resisting projectile and blast impacts, a significant improvement of concrete for protective structure has been observed. Various techniques namely, experimental, analytical and numerical have extensively been investigated in order to predict the resistance of concrete structures under hard projectile impacts.

A review of previous research work reveals that many studies of concrete shelters against dynamic loadings have been conducted from the early 1940s. However, most of the research work ceased shortly after World War II and was not resumed until the 1960s. The resistance of concrete against impact loading is of great interest not only to the designers of defence structures but also to the developers of weapon systems [1-3]. Forrestal used the cylindrical cavity expansion theory to study penetration of rigid rod into dry porous rock and showed that they over predict the early time deceleration response and under-predict the later deceleration response [4]. Forrestal and Luk also showed that the deceleration predictions- from the spherical expansion approximation were in good agreement with the experimental results [5]. Forrestal et al. generalized these models to predict penetration depth into metallic and concrete targets [6], [7].

Semi-empirical two-stage model of Forrestal et al. describing high-speed penetration of an ogive-nosed, rigid projectile into semi-infinite concrete shields and its numerous modifications which have expanded the range of their applications, are widely used in high-speed penetration mechanics [8]. This model includes sub-models for the first stage of penetration (cratering) and the second stage (tunneling).

This paper employs the explicit dynamic finite element code Ls-dyna to analyze how impact loadings affect concrete slabs [9]. Ls-Dyna has several built-in concrete models designed for special purposes such as erosion, effect of strain-rate, cracking, and etc. Among others, the material Type 111 ‘‘Mat-Johnson-Holmquist-Concrete’’ can be used to simulate the large strains, high strain states and high pressures to which the concrete may be subjected [10].

Tham et al. investigated the penetration depth of an ogive-nose projectile into a concrete target using Autodyn-2d and compared their findings with experimental results done by Tai et al. [11], [12]. The purpose of this study is to investigate the penetration of a high velocity ogive–nose shape steel projectile into a semi-infinite concrete target and validate the developed numerical model with experimental results. At the same time penetration depth into concrete target has been calculated using analytical relations developed by Forrestal [8]. These two approaches are then compared with the experimental data.

In the present study, a new analytical model is proposed to predict penetration depth into concrete targets by ogive nose projectiles. In other words, analytical models are modified in order to simulate penetration of a high velocity ogive–nose shape steel projectile into semi-infinite concrete target. Also, Experimental data are used to validate the simulation process. The results of the numerical model and the analytical analyses show good agreement with test results from other researchers.

2 CONSTITUTIVE MODEL

In this study the penetration of an ogive-nose shape steel projectile into a semi-infinite concrete target is simulated. To obtain accurate simulation results, selection of the constitutive model and precision of its inputs are of high importance. The constitutive models used for the steel projectile and concrete target have been simplified by Johnson Cook and Johnson Holmquist; next these models are described briefly.

3 JOHNSON HOLMQUIST MODEL

When concrete is subjected to high velocity impact, it undergoes high pressures, large strains, high strain rates and damage. Therefore, it is necessary to use a material model which includes these effects in the constitutive conditions. In the present study, Holmquist-Johnson-Cook (HJC) material model for concrete (Holmquist et al.) is used in order to mock-up the concrete target [10]. The HJC is an elastic-plastic damage model which considers high strain, strain rate effects and damage. In the HJC (Holmquist et al.) [10] model, the normalized equivalent stress is defined as :

$$\sigma_{eq}^{\ *} = \left[A(1-D) + BP^{*N}\right]\left[1 + C\ln\frac{\dot{\varepsilon}}{\dot{\varepsilon}_0}\right] \quad (1)$$

Where, σ_{eq} is the equivalent stress, f_c is the unconfined compressive strength of concrete, $P^* = P/f_c$ is the normalized pressure, P is the current pressure, $\dot{\varepsilon}$ is the current and $\dot{\varepsilon}_0$ is the reference strain rate. In Eq. (1), normalized cohesive strength A, normalized pressure hardening coefficient B, strain rate coefficient C, pressure hardening exponent N, and normalized maximum strength S_{max} are all material constants. Material damage has also been incorporated using a damage variable D. Stress-pressure relationship

Archive of SID

© 2013 IAU, Majlesi Branch

www.SID.ir

of the material model is presented in Fig. 1. The HJC model uses a strain based damage model, where damage D ($0 \le D \le 1$) is calculated from both the incremental equivalent plastic strain ($\Delta\varepsilon_p$) and the incremental equivalent plastic volumetric strain ($\Delta\mu_p$) which can be expressed as :

$$D = \sum \frac{\Delta\varepsilon_P + \Delta\mu_P}{\varepsilon_P^f + \mu_p^f} \tag{2}$$

Where, the plastic strain to fracture $\Delta\varepsilon_P + \Delta\mu_P$ is defined as :

$$\Delta\varepsilon_P + \Delta\mu_P = \varepsilon_p^f = D_1(p^* + T^*)^{D_2} \ge \varepsilon_{\min}^f \tag{3}$$

Dl and D2 are the damage constants and $T^* = T/f_c$ is the normalized maximum tensile strength. This plastic strain to fracture value is limited by an additional damage constant $\varepsilon_{\min}^f$ in order to limit the plastic strain for material fracture. Damage response of the material model is plotted in Fig. 1 (b).

The pressure-volume behaviour of the HJC concrete model can be expressed in three regions as shown in Fig. 1(c). The linear elastic part is limited by the pressure and volumetric strain values of P_{crush} and μ_{crush}, respectively. In the transition region between the elastic and the total damaged concrete, the material undergoes damage with the presence of plastic volumetric strain. The region ranges from the pressure values P_{crush} to P_{lock}.

At the end of this region, it is assumed that the material is totally damaged and compacted with no tensile strength. The third region defines the fully dense material without any air voids, and the pressure-volume responses at this region is expressed as:

$$p = k_1\bar{\mu} + k_2\bar{\mu}^2 + k_3\bar{\mu}^3 \tag{4}$$

Where k_1, k_2 and k_3 are the material constants, $\bar{\mu} = (\mu - \mu_{lock})/(\mu + \mu_{lock})$ is the modified volumetric strain, $\mu = \rho/(\rho_o - 1)$ is the standard volumetric strain, in which, ρ is the current density and ρ_o is the initial density and $\mu_{lock} = \rho_{grain}/(\rho_o - 1)$ is the locking volumetric strain (where, ρ_{grain} is the grain density). Material properties of the HJC concrete model for plain concrete with compressive strength of 48 MPa are listed in Table 1.

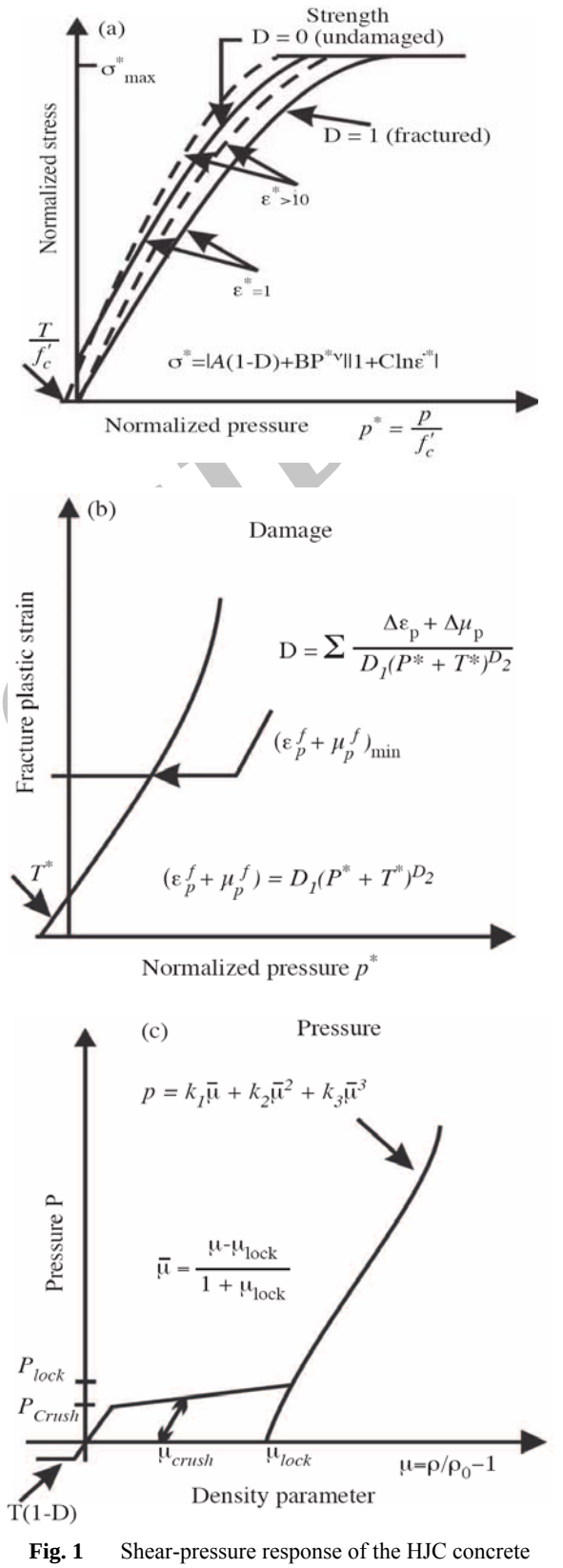

Fig. 1 Shear-pressure response of the HJC concrete model, Holmquist et al. [10]

Archive of SID

© 2013 IAU, Majlesi Branch www.SID.ir

Table 1 Material parameters of the plain concrete (Shiou Tai and Chin Tang) [11]

Numerical Values	Material Properties	Numerical Values	Material Properties
0.75	A	1	D2
1.95	B	2440	$\rho(\frac{kg}{m^3})$
0.007	C	13567	$G\,(MPa)$
0.76	N	48	$f_c\,(MPa)$
17.4	K1 (GPa)	0.001	$(\varepsilon_P^f + \mu_P^f)_{\min}$
38.8	K2 (GPa)	13.6	$P_{crush}\ (MPa)$
29.8	K3 (GPa)	0.000058	μ_{crush}
4	T (MPA)	1.05	$P_{lock}\ (GPa)$
0.03	D1	0.1	μ_{lock}

4 DESCRIPTION OF THE MODEL

Numerical analysis has been employed in dynamic hydro-code of the Ls-Dyna software. To reduce computational effort, a fixed mesh of 4-node two-dimensional (2D) axisymmetric elements (y being the axis of symmetry) is used for both projectile and target. Hourglass option is used to reduce the spurious zero energy modes. To define the conditions of contact between the steel projectile and the concrete target, a 2D automatic-surface-to-surface contact option is used.

$$F = cx \tag{5}$$

$$F = ma = m\frac{d^2x}{dt^2} \tag{6}$$

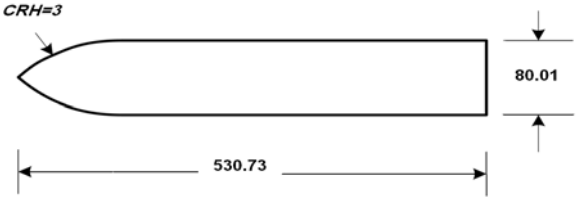

Fig. 2 A typical ogive-nose projectile geometry (CRH-calibre-radius-head) [13]

Although, the projectiles show some pitch and yaw angles for all cases in the experiment, but they were significantly below the critical level and in the current numerical study all the projectile impacts are considered to be normal impacts.

$$x = \frac{v_s}{w}\sin\ wt \tag{7}$$

The ogive-nose steel projectile features a length of 530.73 mm, a diameter of 80 mm and a calibre-radius head (CRH) ratio of 3.0, as shown in Fig. 2 [13].

$$F = \frac{\pi d^2}{4}(sf_c + N\ \ p_c V_1^2) \tag{8}$$

The projectile is assumed to be elastic with following properties:

Mass-density=7800 kg/m^3
Young's modulus=206.9 GPa
Possion's ratio=0.3

As shown in Fig. 3, this analysis employs 72,296 elements and 73,096 nodes.

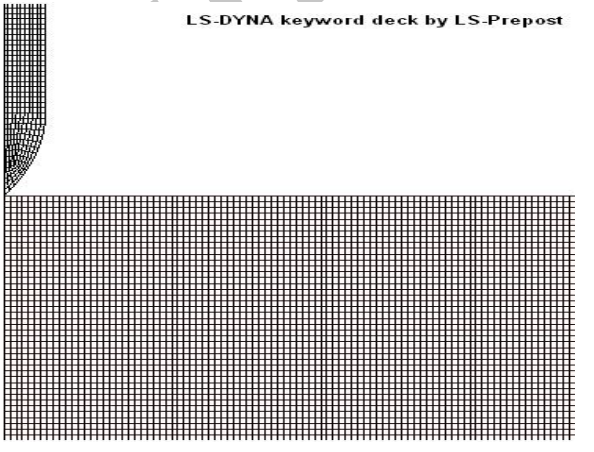

Fig. 3 Projectile and target mesh in Ls-Dyna

5 ANALYTICAL RELATIONS

Forrestal et al. developed an analytical formula to calculate penetration depth of a rigid projectile into concrete target. According to their model, as the projectile penetrates into concrete target, cavity and tunnel regions will be formed in the target. The cavity region is approximately 4 times the radius of the projectile. Here, in the cavity region penetration into target is due to the surface effect. The tunnel region starts from the end of the cavity and continues up to the final penetration depth. Here, spherical cavity expansion theory, developed by Bishop and later used by Forrestal et al., to calculate normal stress on the nose of the projectile, has been used to calculate the force exerted on the nose of the projectile [7], [8], [15]. Now, using the model presented by Forrestal the final crater depth in concrete can be calculated [8], [14].
Since acceleration of projectile is considered to be linear, the axial force on the nose of the projectile in the cavity region can be estimated as

© 2013 IAU, Majlesi Branch
www.SID.ir

$$F = cx$$

Where c is a constant and x is the depth of penetration in a crater region measured from the concrete surface. From the Newton's second law, with the initial condition at $t = 0$: $x = 0$, and $v = v_s$; the above equation has the following solution for the projectile penetration depth.

$$w = \sqrt{\frac{c}{m}} \tag{9}$$

Where 'c' is a constant for 0< x< 4a. The unidentified constant c is obtained from the conditions of continuity of force, velocity, and displacement at x= 4a. The force on the penetrating nose is expressed by Ref. [4]. p_c is the density of concrete target, and V_1 is the rigid body projectile velocity at x=4a. Where 'a' is the projectile shank radius, S the dimensionless parameter which depends on unconfined compressive strength of concrete, from Ref. [4].

$$S = 82.6\, f_c^{-0.544} \tag{10}$$

N is a dimensionless constant that depends on the projectile calibre radius head ψ, which is estimated as

$$N = (8\psi - 1)/24\psi^2 \tag{11}$$

Substituting Eq. (5) in the right-hand side and Eq. (3) in the left-hand side of, Eq. (2) we get

$$mwv_s \sin wt_1 = -\frac{\pi d^2}{4}(sf_c + N\ p_c V_1^2) \tag{12}$$

The velocity at the interface of crater and tunnel region (i.e., x=4a) is :

$$\frac{dx}{dt} = v_c \tag{13}$$

Substituting Eq. (3) into Eq. (9), we get

$$4a = \frac{V_0}{w}\sin w_1 t \tag{14}$$

Substituting Eq. (10) into Eq. (8) gives

$$V_1 = \sqrt{\frac{mVs^2 - 4\pi a^3 Sf_c}{m + 4a^3 \pi N p_c}} \tag{15}$$

Where, V_1 is the entrance velocity from the cavity to the tunnel. Using the Newton's second law and Eq. (5), the tunnel region is given by:

$$m\frac{d^2 z}{dt^2} = m\frac{Vdv}{dz} = -\pi a^2 (sf_c + NpV^2) \tag{16}$$

In the tunnel region, assuming that the projectile enters tunnel region of the concrete target, and integrating Eq. (12) in tunnel region, the final penetration depth is calculated as :

$$X = \frac{2M}{\pi d^2 N\ P_C}\ln(1 + \frac{NP\ V_1^2}{Sf_c}) + 4a \tag{17}$$

Integrating equation (12) from V_c to zero and 4a to Z_t, gives the residual velocity as,

$$\frac{-m}{\pi a^2 Sf_c}\int_{V_c}^{0} \frac{Vdv}{(1 + \frac{NpV^2}{Sf_c})} = \int_{4a}^{Z_t} dz \tag{18}$$

$$V_n^2 = \frac{Sf_c}{Np}\{\exp[\frac{(z_t - z_c)(2\pi a^2 Np)}{m_p + m_c} - 1]\} \tag{19}$$

Where z_t is the thickness of the concrete target, m_p is the projectile mass, and m_c is calculated as :

$$m_C = \pi a^2 z_C p \tag{20}$$

Where m_c is the mass of concrete particles, ρ is mass density of concrete target, 'a' is Shank radius of the projectile, and z_c is penetration depth of the projectile in crater region. Substituting from Eq. (15) into Eq. (11) gives the residual velocity as,

$$V_B = \sqrt{\frac{V_n^2(m + \pi a^2 NpZc) + \pi a^2 Sf_c Z_C}{m}} \tag{21}$$

When the rigid projectile impacts the target, the target absorbs kinetic energy of the projectile. Therefore, using the principal of conservation of energy and the forces acting on the projectile between the cavity and the tunnel will results in,

Archive of SID

© 2013 IAU, Majlesi Branch www.SID.ir

$$F = \frac{mV_B^2}{(Zt - Zc)} \tag{22}$$

This is the equation of conservation of energy written between the crater region and the final penetration region.

$$mV_S^2 = FH \tag{23}$$

Where, H is final penetration and V_s is the impact velocity. Final penetration depth is calculated as

$$Z = 2d + H \tag{24}$$

6 RESULTS AND DISCUSSION

Table 2 shows the experimental results, the simulation results, as well as the analytically computed results. The results of the experiment and analytical formula in the present study, in velocity range of 200 to 378.6 m/s, are very close. This indicates that an analytical formula may be used with a good degree of confidence in order to estimate the experimental outcome of penetration depth of a rigid projectile into concrete targets [14].

Table 2 Comparison of experimental results with simulated and analytical results

Simulated Penetration Depth (m)	Analytical Penetration Depth (m)	Experimental Penetration Depth (m)	Impact Velocity (m/s)
0.46	0.3964	0.42	200
0.98	0.9254	0.93	336.6
1.19	1.179	1.18	378.6

Fig. 4 shows the comparison between the experimental, analytical, and numerically simulated results. This figure points out good agreement between the results and also indicates the degree of reliability of the analytical and the numerical results. Fig. 5 shows the comparison between experimentally measured penetration depth using numerical simulation as well as the results extracted from the analytical formulation. Where velocities are less than 500 m/s, the results are very close; however, at velocities higher than 500 m/s, the difference between simulation and experimental result increase, which may be due to the fact that Forrestal has not taken into account the projectile nose deformation. Fig. 5 also shows that the calculated and simulated penetration depths are the upper and lower limits of the experimental results, respectively. This makes it possible to optimize the design of a penetrator into concrete target using the results of the analytical formula as well as the simulation process.

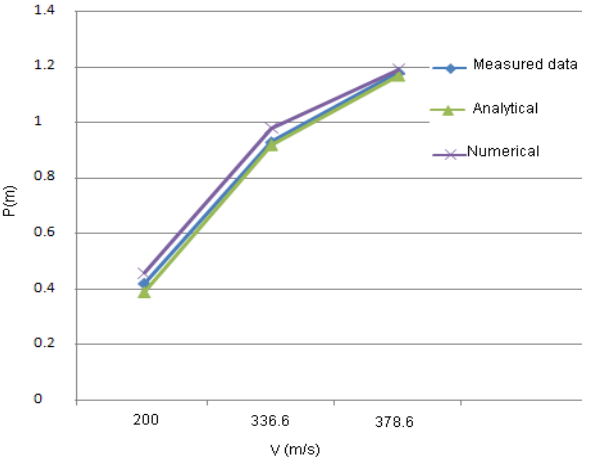

Fig. 4 Comparison of experimental, analytical, and numerical results

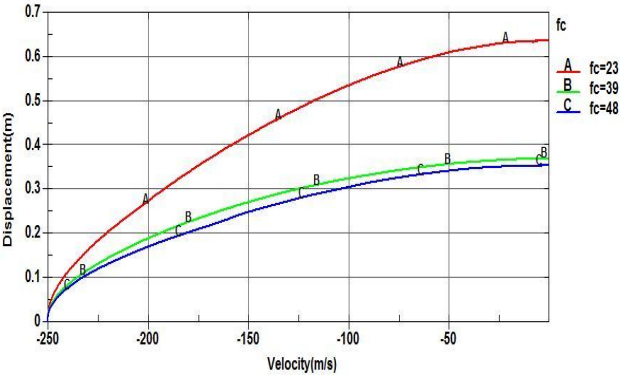

Fig. 5 Comparison of impacts for: (A) CRH = 1.5; (B) CRH = 3.0; and (C) CRH =4.25

6.1. Effect of CRH ratio for steel projectiles

It is anticipated that the CRH (calibre-radius-head) ratio of the ogive-nose projectile may be an important factor influencing the behavior of concrete under impact loading. In this section, the effects of CRH values of the ogive-nose projectile are numerically investigated. In our calculations, the total length and the diameter of the projectile are assumed to be constant. Four values of CRH=1.5, 3.0, 4.25, 6 (namely CRH1, CRH2, CRH3 and CRH4) are considered in order to explore the effect of CRH ratio on the projectile impact on concrete. Fig. 5 compares the simulated results of the four values of CRH at an impact velocity of 378.6 m/s. It clearly demonstrates that, the higher the value of CRH is, a deeper penetration can be expected.

Archive of SID

© 2013 IAU, Majlesi Branch

www.SID.ir

6.2. Effect of unconfined compressive strength on concrete targets

Fig. 6 compares the simulated results of the unconfined compressive strength of concrete targets at an impact velocity of 250 m/s with 23, 39 and 48 MPa and target diameter of D=1.83 m. Obviously with the increase in the unconfined compressive strength of concrete target, depth of penetration will decrease.

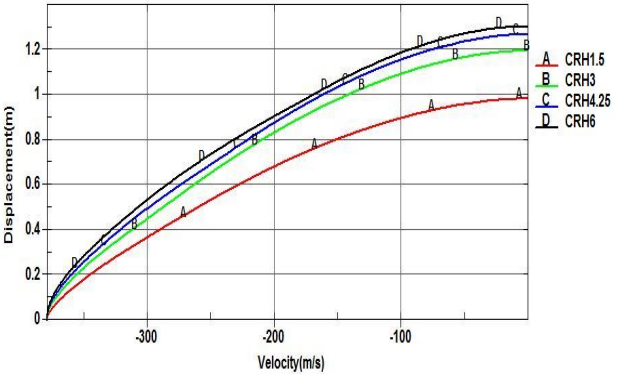

Fig. 6 Effect of unconfined compressive strength of concrete targets on the depth of penetration for: (A) CRH = 1.5; (B) CRH = 3.0; (C) CRH =4.25; and (D) CRH = 6.0

7 CONCLUSION

Perforation of high-velocity objects through structural concrete is one of the most challenging problems for designers in civil defense engineering. In this article, a new analytical model is proposed to predict penetration depth into concrete target by ogive nose projectiles. The results of the analytical model were compared with simulation results and also the experimental results of Ref. Forrestal [6]. The results show that a very close agreement does indeed exist between the simulation model, the analytical model, and the experimental results.

REFERENCES

[1] Kennedy, R. P., "Review of procedures for the analysis and design of concrete structures to missile impact effects", Nucl Eng 1976, Vol. 37, No. 2, pp. 183-203.

[2] Balandin, D. V., Bolotnik, N. N., and Pilkey, W. D., "Optimal protection from impact, shock, and vibration", Toronto: Gordon and Breach Science Publisher, 2001.

[3] Teng, T. L., Chu, Y. A., Chang, F. A., and Chin, H. S., "Numerical analysis of oblique impact on reinforced concrete", Cement Concrete Compos 2005, Vol. 27, No. 4, pp. 481-92.

[4] Forrestal, M. J., "Penetration into dry porous rock", Internat. J. Solids and Structures 22, 1986, pp. 1485-1500.

[5] Forrestal, M. J., Luk, V. K., Rosenberg, Z., and Brar, N. S., "Penetration of 7075-T651 aluminum targets with ogival-nose rods", Int. J. Solids Struct. Vol. 29, 1992, pp. 1729-1736.

[6] Forrestal, M. J., Tzou, D. Y., Askari, E., and Longcope, D. B., "Penetration into ductile metal targets with rigid spherical-nose rods", Int. J. Impact Eng. 16, 1995, pp. 699-710. (1995).

[7] Forrestal, M. J. and Tzou, D. Y., "A Spherical Cavity-Expansion Penetration Model for Concrete Targets", Int. J. Solids and Structures, Vol. 34, 1997, pp. 4127-4146.

[8] Forrestal, M. J., Altman, B. S., Cargile, J. D., and Hanchak, S. J., "An empirical equation for penetration depth of ogive-nose projectiles into concrete target", Int J Impact Eng., Vol. 15, No. 4, 1994,:pp. 395-405.

[9] Livemore Software Technology Corporation (LSTC). LS-DYNA Keyword User's manual, California, USA; 2003.

[10] Holmquist, T. J., Johnson, G. R., and Cook, W. H., "A Computational Constitutive Model for Concrete Subjected to Large Strains, High Strain Rates, High Pressure", 14th international Symposium on Ballistics, Qucbec, 1993, pp. 591-661.

[11] Tham, C. Y., "Numerical and Empirical Approach In Predicting of a Concrete Target by an Ogive-Nosed Projectile", Int. J. Finite Element in Analysys and Dsign. 42, 2006, pp. 1258-1268.

[12] Tai, Y. Sh., and Tang, Ch. Ch., "Numerical simulation: The dynamic behavior of reinforced concrete plates under normal impact", Int. J. Theoretical and applied fracture mechanics, 2006, pp. 117-127.

[13] Frew, D. J., Forrestal, M. J., and Cargile, J. D., "The effect of concrete target diameter on projectile deceleration and penetration depth", Sandia National Laboratories, Albuquerque, NM 87185-0325, USA.

[14] Forrestal, M. J., Frew, D. J., Hickerson, J. P., and Rohwer, T. A., "Penetration of concrete targets with deceleration-time measurements", Int J Impact Eng, Vol. 28, 2003, pp. 479-97.

[15] Bishop, R. F., R. Hill and N. F. Mott, "The theory of Indentation Hardness tests", Proc. Phys. Soc. Vol. 57, 1945, pp. 147-159.

Archive of SID

© 2013 IAU, Majlesi Branch www.SID.ir